

Evidence of Non-Linear Relationship Between the Electrical Conductivity of Y₂O₃-Stabilized-ZrO₂ in the Low Temperature Range

WEI ZHAO, IK JIN KIM* and JIANGHONG GONG†

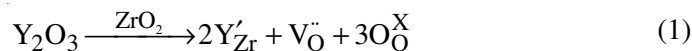
*Department of Materials Science and Engineering, Institute for Processing and Application of Inorganic Materials (PAIM), Hanseo University, South Korea
E-mail: ijkim@hanseo.ac.kr*

The relationship between the electrical conductivity and temperature of Y₂O₃-Stabilized-ZrO₂ (YSZ) electrolyte samples in the lower temperature range was examined by complex impedance measurements at temperatures between 363 and 733 K. There was a non-linear relationship between the electrical conductivity and temperature. The former decreased gradually at a decreasing rate with decreasing temperature. This paper presents evidence supporting these results.

Key Words: Electrical conductivity, Y₂O₃-Stabilized-ZrO₂, Electrolyte, Complex Impedance, Activation energy.

INTRODUCTION

Since Nernst reported yttria (Y₂O₃)-doped zirconia (ZrO₂) in 1899¹ and Wagner² explained the principle of ionic conduction in stabilized ZrO₂, there have been many studies on the properties of stabilized ZrO₂. ZrO₂ fully stabilized by Y₂O₃ is an oxide system with the fluorite structure. In addition to stabilizing the fluorite structure, doping also causes the formation of oxygen vacancies as charge-compensating defects depicted by the following formula:



Because of its high oxygen ion conductivity and chemical stability, stabilized cubic ZrO₂ is considered to be an excellent electrolyte material in solid oxide fuel cells (SOFCs) and many sensor applications. Consequently, during the past few decades, the electrical properties of Y₂O₃-stabilized ZrO₂ (YSZ) have been studied extensively³⁻⁷.

According to the extensive researches on the YSZ electrolyte, YSZ electrolyte is a type of electrolyte material used in high temperature solid oxide fuel cells (SOFCs) which usually is used in SOFCs operating between 1173 and 1273 K. However, the request for a material in this range is too strict and severe. Therefore, an examination of its properties at lower temperatures is necessary.

†Department of Materials Science and Engineering, Tsinghua University, Beijing 100084, P.R. China.

In this study, the properties of YSZ in the lower temperature range were examined using complex impedance tests.

EXPERIMENTAL

All the samples examined had the same nominal chemical composition of $(\text{ZrO}_2)_{0.96}-(\text{Y}_2\text{O}_3)_{0.08}$ which can be described by 8YSZ (8 means that the mole fraction of Y_2O_3 is 8 %). To prepare these samples, analytical ZrO_2 powder (99.5 % purity) and Y_2O_3 powder (> 99.5 % purity) were mixed at the desired ratio and wet-milled with ZrO_2 balls for 12 h in a plastic pot. After the powder mixtures were dried, disc-shaped compacts, 10 mm in diameter with different thicknesses ranging from 150 μm -1.2 mm, were green-formed by die-pressing and isostatically pressed at approximately 200 MPa. The samples were then sintered in air at 1873 K for 2 h and furnace-cooled to room temperature. To realize a regular change of the thickness between sintered samples, they all were polished mechanically until anticipated thicknesses were obtained. Because of the same error standard caused by polishing, all samples were reasonably comparable. Table-1 lists all the samples and their designations in this study.

TABLE-1
SAMPLES WITH DIFFERENT THICKNESSES OF INTEREST

Sample code	A	B	C	D
Thickness (μm)	992	643	389	160

Characterization of the test samples: The sintered samples were characterized by X-ray diffraction (XRD) with $\text{Cu K}\alpha$ radiation. XRD indicated all the samples to be a single phased fluorite-type solid solution with cubic symmetry and no other phases.

The geometric density of the sintered samples was measured using the conventional Archimedes method. The relative density was determined as the ratio of the true density to its theoretical value. The values showed that the relative densities of all samples were ≥ 93 %. Therefore, it can be inferred that all samples were sufficiently dense.

Scanning electron microscopy (SEM) was also used to confirm the results of the density tests. Although some pores between the grains could be observed, they were not believed to deteriorate the properties.

A platinum paste was applied as electrodes to both sides of the samples by firing at 1373 K for 0.5 h after they had been polished slightly. The electrical contacts were made with silver wires with an appropriate length. The complex impedance spectra of the sintered samples were measured using a computer-controlled frequency response analyzer (HP4194A, Hewlett-Packard, CA). The measurement was carried out in air at temperatures ranging from 363-733 K, at intervals of approximately 20 K and over the frequency range, 10^2 - 10^7 Hz. Two systems of HP4194A analyzer/heater were employed, one for the temperature range from 363-473 K and the other

for the temperature range from 473-733 K. As will be shown below, there are slight differences between the results measured from the two systems.

RESULTS AND DISCUSSION

Basic knowledge about the electrical conductivity: Generally, complex impedance plots of polycrystalline solid electrolytes show three characteristic semicircles, which represent the electrode effects, grain-boundary effects and lattice effects with decreasing frequencies⁸. In most applications of doped ZrO₂, it is usually present in polycrystalline form. In this study, a well-defined semicircle due to the lattice and only a part of the semicircle due to the grain boundary were observed in the lower temperature range. Mostly, within almost the entire temperature range of this study, the semicircles due to the grain-boundary effects could be detected and the characteristic frequencies were sufficiently different to allow good separation between this semicircle and the one due to the lattice. Fig. 1 shows typical examples of the measured complex impedance plots.

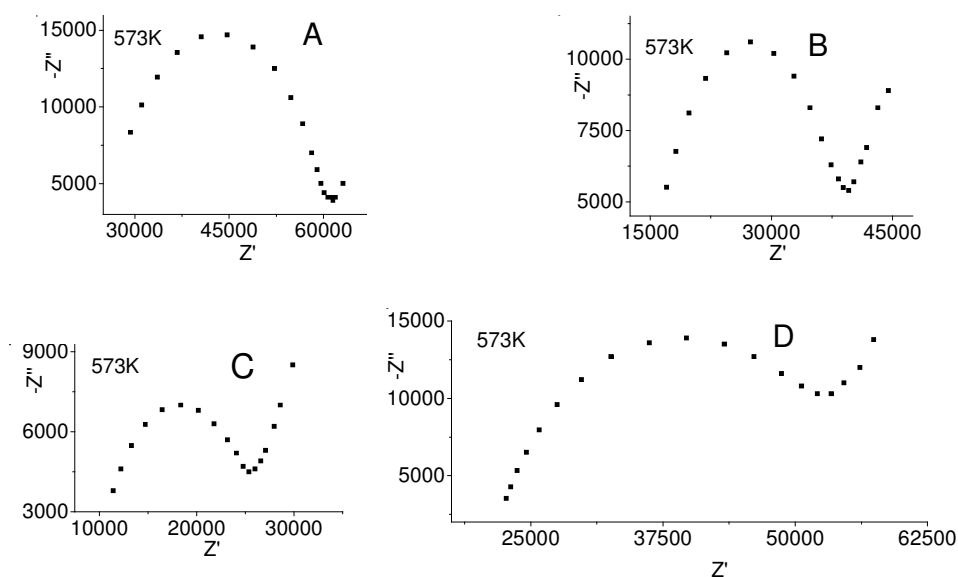


Fig. 1. Typical complex impedance plots measured at 573 K for samples (A), (B), (C), (D)

Following the pioneering work of Bauerle in 1969⁹, the lattice resistance R_g and the grain boundary resistance R_{gb} were extracted from the measured complex impedance plots for each sample at almost every temperature investigated. Each extracted resistance datum R was formally converted to a conductivity datum σ , using the following equation:

$$\sigma = \frac{t}{SR} \quad (2)$$

where S represents electrode area and t stands for thickness of the sample surface. In this way, the apparent lattice conductivity $(\sigma_g)_a$ and apparent grain-boundary conductivity $(\sigma_{gb})_a$ can be obtained through these complex impedance plots.

In all circumstances, the value of $(\sigma_g)_a$ may be treated approximately as the true value due to the negligibly small thickness of the grain-boundary layers in the samples. In addition, determining the true values of $(\sigma_{gb})_a$ requires extensive microstructural measurements, which are to characterize the grain-boundary geometry. For this study, this measurement appears to be unnecessary. Here the lattice conductivity is the main focus.

Temperature dependence of lattice conductivity: It is well-known that the correlation between temperature and conductivity can be described by the classical Arrhenius equation¹⁰:

$$\sigma = A' \exp\left(-\frac{E}{\kappa T}\right) \quad (3)$$

where T is the absolute temperature, κ represents the Boltzman constant and A' and E denote the pre-exponential factor and activation energy, respectively. By reorganizing eqn. 3, a new formula that demonstrates a linear relationship between $\ln(\sigma T)$ and $1/T$ can be obtained as follows:

$$\ln(\sigma T) = \ln A' - \frac{E}{\kappa T} \quad (4)$$

This is a linear equation in the simple form of $y = ax + b$, where y , x , a , b are referred to as $\ln(\sigma T)$, $10^4/T$, $\ln(A')$ and $(-E/10^4\kappa)$, respectively. Fig. 2 shows the $\ln(\sigma T)$ - $10^4/T$ plots for all corresponding samples in this study.

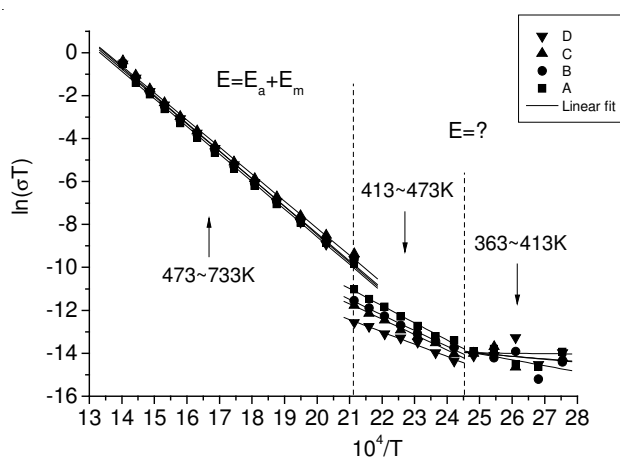


Fig. 2. $\ln(\sigma T)$ - $10^4/T$ plots for all corresponding samples

It is clear from Fig. 2, the relationship is non-linear over the entire temperature range. It is very different from the result obtained from eqn. 4. However, it is strictly a linear relationship at each of the three temperature intervals. Therefore, the

relationship described by the Arrhenius formula is not universal over the entire temperature range of interest but reasonable for the appropriate temperature intervals. It is noted that the plot breaks at 473 K, the reason for which is the relatively large error caused by the testing machine within the temperature range below 473 K. Despite that, the results are still reasonable.

This non-linear behaviour is similar to the results reported by many researches since the mid 1980s¹¹⁻¹⁴. Despite the similarity, there is little difference between them, *i.e.*, the tendency of the slopes of the lines. In this study, the slopes of the lines in Fig. 2, which represent the activation energies for lattice conduction, decrease with increasing temperature. There is an ideal explanation for the conduction of oxygen vacancies.

Theoretically, the carriers in YSZ electrolytes can be classified into two types, free vacancies and associated ones. The percentage of them in the whole solid material can be assumed to be x and $(1-x)$, respectively. Based on theoretical calculations, the migration enthalpy E_m for the former is approximately 0.8 eV¹⁵ and the associated enthalpy E_a for the latter is approximately 0.26 eV¹⁶. The activation energy (E) of the material can be obtained using the following equation:

$$\begin{aligned} E &= (1 - x)(E_m + E_a) + xE_m \\ &= E_m + (1 - x)E_a \end{aligned} \quad (5)$$

Therefore, at higher temperatures, the lattice vibration is intense enough to make free vacancies dominant and E may be equal to E_m ¹⁷. In other words, x in eqn. 5 is unity, while at lower temperatures, almost all the oxygen vacancies are bound by the interaction between them and the doping cations. Therefore, x is approximately zero and E may be equal to $E_m + E_a$, which is 1.06 eV.

From the explanation above, it is easy to obtain two inferences which are (1) the activation energy E will be not less than 0.8 eV, even at lower temperatures and (2) the activation energy will increase with decrease in the temperature. Compared with the results in Table-2, the inferences are quite different from the values calculated in this study. First, although the values at 473-733 and 363-413 K may be considered to be in accordance with the theoretically-calculated values, the data at 413-473 K is already much less than 0.8 eV and all the samples confirm that the result is not a coincidence. Furthermore, it is obvious that the activation energy decreases with decrease in the temperature. Therefore, the theory does not appear to explain the results in this study.

Although the ideal theory¹⁸ cannot be a perfect interpretation of the results in this study, it is difficult to say that the theory is incorrect because it is the interpretation that leads to a study of a further stage. It must be noted that the assumption¹⁹ of the theory concentrates on the ideal and extreme state of the carriers. It assumes that electrical conduction involves all oxygen vacancies, which are all free at higher temperatures, while the vacancies are all associated ones at lower temperatures. Strictly speaking, this is unsuitable for the case at much lower temperatures. When considering that at absolute zero, the energy of all particles decreases to zero, so

TABLE-2
ACTIVATION ENERGY IN DIFFERENT TEMPERATURE
RANGES FOR ALL SAMPLES

Thicknesses of the samples (t/ μm)	Activation energy in different temperature ranges (E/eV)		
	473-733 K	413-473 K	363-413 K
A	1.13	0.49	0.02
B	1.10	0.62	0.12
C	1.11	0.63	0.24
D	1.11	0.69	0.10

the conductivity is also zero. When the temperature increases gradually, the lattice vibrations will become stronger and the energy of the particles will begin to increase so that they can migrate. From the viewpoint of statistical physics, the theoretical values of E_m and E_a should just be statistical, which means that they are not the same for real materials at different temperatures. With an increase in the temperature, some vacancies with a lower associated energy will begin to be activated, resulting in more free oxygen vacancies. Therefore, at lower temperatures, only the vacancies with a lower migration energy can contribute to the electrical conduction. Consequently, in addition to the increase in temperature in the lower temperature range (in this study it is between 363 and 733 K), E_m and E_a should increase to a maximum at a certain temperature.

Important support for the above comes from the report by Orliukas *et al.*²⁰, who analyzed the concentration of effective carriers in solid electrolytes using the following equation:

$$n = \frac{6k}{z^2 e^2 d^2 \gamma} \left(\frac{\sigma T}{\omega_p} \right) \quad (6)$$

where z ($= 2$), e ($= 1.6 \times 10^{19}$ A s), d , $\omega_p = 2\pi f_p$ represent the charge number of the carriers, the quantity of electric charge, average transition distance of carriers and characteristic relaxation frequency of the material, respectively. γ is a modified factor. According to the analysis reported by Li *et al.*¹⁸, through the calculation of σ and f_p , the change in the effective carrier concentration with temperature. Fig. 3 confirms the previous analysis, which is basically in accordance with Boltzmann distribution theory.

Some other characteristics of the $\ln(\sigma T) - 10^4/T$ plots: According to Hohnke's analysis²¹, there is a linear relationship between $\ln A'$ and the activation energy E for many binary systems that involve ZrO_2 . The experimental data shown in Fig. 4 appears to indicate that the empirical formula:

$$\ln A' = aE + b \quad (7)$$

is also suitable for the system investigated in this study. The values for a and b in different temperature ranges were obtained by linear regression calculation.

Through Hohnke's analysis, the slope a of the $\ln A' - E$ straight-line plot corresponds to $1/(\kappa T_0)$, where T_0 is a characteristic temperature at which all Arrhenius

plots (*i.e.*, $\ln(\sigma T) - 10^4/T$ curves) for all samples in a given system will converge. Gong *et al.*²² reported the calculated value of T_0 for their ternary system was *ca.* 1060 K within the high temperature range.

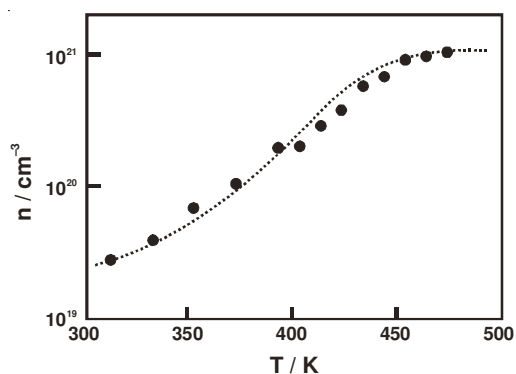


Fig. 3. Variation of the effective carrier concentration with temperature¹⁸

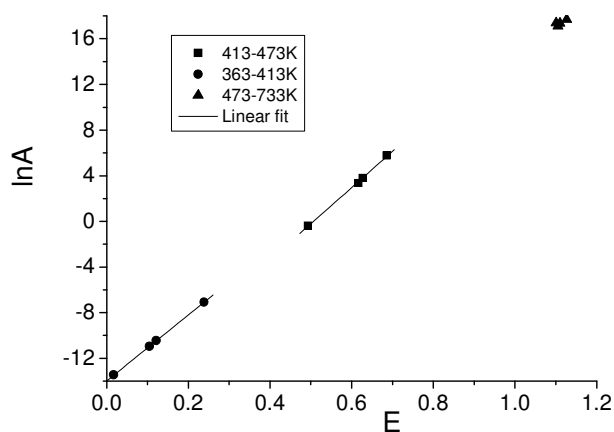


Fig. 4. Plot of the relationship between the pre-exponential factor A' and the activation energy E

In this study, a little different from that of Gong *et al.* has been obtained by calculation, which is that all straight lines discussed within the range of 473-733 K tend to converge at approximately 667 K. Although certain plots in this temperature range do not cross this temperature point, most of the plots converge at this temperature, which confirms the theoretically calculated result.

Interestingly, all the plots within ranges of both 363-413 and 413-473 K tended to converge at the same temperature point between 365 and 401 K, as shown in Fig. 2. Therefore, by integrating both results, there is more than one convergence within a large temperature range involving high, intermediate and low temperatures. This study found a new convergence within the lower temperature range.

Conclusion

The linear relationship between the electrical conductivity and temperature inferred from the Arrhenius formula is not universal over the entire temperature range but is applicable in distinct intervals. Therefore, a non-linear relationship was found between them. An explanation based on the ideal theory mentioned above was proposed in that within the low temperature range, the activation energy corresponding to the slope of $\ln(\sigma T) - 10^4/T$ plots increases with an increase in the temperature. This is in contrast to many results reported previously, even though it can explain the phenomenon well. The pre-exponential factor and activation energy are two important parameters affecting the electrical conductivity and they should be considered simultaneously. A new convergence within the lower temperature range was found from the $\ln(\sigma T) - 10^4/T$ plots along with the calculation.

REFERENCES

1. W. Nernst, *Z. Electrochem.*, **6**, 41 (1900).
2. C. Wagner, *Naturwissenschaften*, **31**, 265 (1943).
3. A.I. Ioffe, D.S. Rutman and S.V. Karpachov, *Electrochim. Acta*, **23**, 141 (1978).
4. S.P.S. Badwal, *J. Mater. Sci.*, **19**, 1767 (1984).
5. X. Li and B. Hofskjold, *J. Phys. D*, **7**, 1255 (1995).
6. A. Pimenov, J. Ullrich, P. Lunkenheimer, A. Loidl and C.H. Ruscher, *Solid State Ionics*, **109**, 111 (1998).
7. J. Luo, D.P. Almond and R. Stevens, *J. Am. Ceram. Soc.*, **83**, 1703 (2000).
8. P. Abélard and J.F. Baumard, *Pure Appl. Chem.*, **67**, 1891 (1995).
9. J.E. Bauerle, *J. Phys. Chem. Solids*, **30**, 2657 (1969).
10. T.H. Etsell and S.N. Flengas, *Chem. Rev.*, **70**, 339 (1970).
11. J.E. Bauerle and J. Hrizo, *J. Phys. Chem. Solids*, **30**, 565 (1969).
12. P. Abélard and J.F. Baumard, *Phys. Rev.*, **26B**, 1005 (1982).
13. J.D. Solier, M.A. Pérez-Jubindo, A. Dominguez-Rodriguez and A.H. Heuer, *J. Am. Ceram. Soc.*, **72**, 1500 (1989).
14. S.P.S. Badwal, *J. Am. Ceram. Soc.*, **73**, 3718 (1990).
15. W.C. Mackrodt and P.M. Woodrow, *J. Am. Ceram. Soc.*, **69**, 277 (1986).
16. V. Butler, C.R.A. Catlow and B.E.F. Fender, *Solid State Ionics*, **5**, 539 (1984).
17. A.S. Nowick, In: *Diffusion in Crystalline Solids*. Orlando: Academic, pp. 143-188 (1984).
18. Ying Li, Jianghong Gong, Yusheng Xie, Zilong Tang, Yunfa Chen and Zhongtai Zhang, *J. Inorg. Mater.*, **17**, 811 (2002).
19. J.A. Kilner and B.C.H. Steel, In: *Nonstoichiometric Oxides*. New York: Academic Press, pp. 233-269 (1981).
20. A. Orliukas, P. Bohac, K. Sasaki and L.J. Gauckler, *Solid State Ionics*, **72**, 35 (1994).
21. D. K. Hohnke, In: *Fast Ion Transport in Solids*. Noth-Holland, Amsterdam, The Netherlands, pp. 669-672 (1979).
22. J.H. Gong, Y. Li, Z.T. Zhang and Z.L. Tang, *J. Am. Ceram. Soc.*, **83**, 648 (2000).

(Received: 10 December 2009;

Accepted: 4 June 2010)

AJC-8767